Electromagnetic signatures of chiral quantum spin liquid

Saikat Banerjee
Theoretical Division, T-4, Los Alamos National Laboratory, Los Alamos, New Mexico 87545, USA

Wei Zhu
School of Science, Westlake University, 18 Shilongshan Road, Hangzhou 310024, China and
Institute of Natural Sciences, Westlake Institute for Advanced Study, 18 Shilongshan Road, Hangzhou 310024, China

Shi-Zeng Lin
Theoretical Division, T-4 and CNLS, Los Alamos National Laboratory, Los Alamos, New Mexico 87545, USA and
Center for Integrated Nanotechnologies (CINT), Los Alamos National Laboratory, Los Alamos, New Mexico 87545, USA

CONTENTS

I. HUBBARD MODEL TO CHIRAL SPIN MODEL

In this section, we outline the steps for phenomenologically obtaining the chiral spin model starting from a Hubbard model on a triangular lattice at half-filling. The corresponding Hamiltonian is written as

$$\mathcal{H} = -t \sum_{\langle ij\rangle,\sigma} c^\dagger_{i\sigma} c_{j\sigma} + U \sum_i n_{i\uparrow} n_{i\downarrow}, \tag{1}$$

where $\langle ij\rangle$ corresponds to the nearest-neighbor tight-binding model on a triangular lattice, σ corresponds to the spin degrees of freedom, and U is the strength of the local Hubbard repulsion. In this case, the low-energy effective spin Hamiltonian in the strong-coupling limit ($U \gg t$) can be obtained through Schrieffer-Wolff transformation (SWT) [1, 2] as

$$\mathcal{H}_{\text{eff}} = \mathcal{H}^{(2)}_{\text{eff}} + \mathcal{H}^{(4)}_{\text{eff}}, \quad \mathcal{H}^{(2)}_{\text{eff}} = J^{(2)} \sum_{\langle ij\rangle} \mathbf{S}_i \cdot \mathbf{S}_j, \tag{2a}$$

$$\mathcal{H}^{(4)}_{\text{eff}} = J^{(4)}_1 \sum_{\langle ij\rangle} \mathbf{S}_i \cdot \mathbf{S}_j + J^{(4)}_2 \sum_{\langle\langle ij\rangle\rangle} \mathbf{S}_i \cdot \mathbf{S}_j + J^{(4)}_3 \sum_{\langle\langle\langle ij\rangle\rangle\rangle} \mathbf{S}_i \cdot \mathbf{S}_j + J^{(4)}_{\text{R}} \sum_{\langle i,j,k,l\rangle} \mathcal{R}_{ijkl}, \tag{2b}$$

$$\mathcal{R}_{ijkl} = (\mathbf{S}_i \cdot \mathbf{S}_j)(\mathbf{S}_k \cdot \mathbf{S}_l) + (\mathbf{S}_i \cdot \mathbf{S}_l)(\mathbf{S}_j \cdot \mathbf{S}_k) - (\mathbf{S}_i \cdot \mathbf{S}_k)(\mathbf{S}_j \cdot \mathbf{S}_l), \tag{2c}$$

where the exchange couplings are given by [2]

$$J^{(2)} = \frac{4t^2}{U}, \quad J^{(4)}_1 = -\frac{24t^4}{U^3}, \quad J^{(4)}_2 = J^{(4)}_3 = \frac{4t^4}{U^3}, \quad J^{(4)}_{\text{R}} = \frac{80t^4}{U^3}. \tag{3}$$

In a previous theoretical work [3], it was shown that the ring exchange term leads to an induced chirality in the low-energy spin dynamics of the TLHM. It is worth mentioning that such a flux phase was previously pointed out in triangular lattice material κ-$(\text{ET})_2\text{Cu}_2(\text{CN})_3$ by Motrunich within the mean-field description in Ref. [4]. Motivated by these studies, we consider the following chiral spin liquid model as

$$\mathcal{H}_{\text{pheno}} = \tilde{J} \sum_{\langle ij\rangle} \mathbf{S}_i \cdot \mathbf{S}_j + \tilde{J}_\chi \sum_{\substack{\langle\langle ijk\rangle\rangle \\ \triangle,\triangledown}} \mathbf{S}_i \cdot (\mathbf{S}_j \times \mathbf{S}_k), \tag{4}$$

where $\tilde{J}$, and $\tilde{J}_\chi$ are provided in Ref. [3] as

$$\tilde{J} = J^{(2)} - \frac{107}{88} J^{(4)}_{\text{R}}, \quad \tilde{J}_\chi = 3J^{(4)}_{\text{R}} \left(-\frac{39}{11}\chi - \frac{1344}{11}\chi^3 + \frac{12288}{11}\chi^5 \right), \tag{5}$$

where $\chi = \langle \mathbf{S}_i \cdot (\mathbf{S}_j \times \mathbf{S}_k)\rangle$ is the non-vanishing chiral order parameter in the emergent chiral QSL state. Self-consistent density-matrix renormalization analysis in Ref. [3, 5] shows that it is non-vanishing in a wide region between $U_{\text{c}_1} \sim 9U$ and $U_{\text{c}_2} \sim 10.75U$. Therefore, the parameters of the phenomenological Hamiltonian in the main text are directly related to the parameters of the original Hubbard model.

II. PHENOMENOLOGICAL DESCRIPTION

We assume that the underlying fractionalized excitations are spinons, and correspondingly rewrite the spin degrees of freedom as [6] $\mathbf{S}_i = \frac{1}{2} f^\dagger_{i\alpha} \boldsymbol{\sigma}_{\alpha\beta} f_{i\beta}$. Here, $f^\dagger_{i\alpha}$ creates a spinon at site i with spin α, and $\boldsymbol{\sigma}$ denotes the vector of the Pauli matrices. We utilize the product relation for the Pauli matrices as

$$\boldsymbol{\sigma}_{\alpha\beta} \cdot \boldsymbol{\sigma}_{\gamma\delta} = 2\delta_{\alpha\delta}\delta_{\beta\gamma} - \delta_{\alpha\beta}\delta_{\gamma\delta}. \tag{6}$$

Plugging this back into Eq. (3) of the main text, we first obtain the Heisenberg part as

$$\mathcal{H}_{\text{heisen}} = -\frac{\tilde{J}}{2} \sum_{\langle ij\rangle} f^\dagger_{i\alpha} f_{j\alpha} f^\dagger_{j\beta} f_{i\beta} - \frac{\tilde{J}}{4} \sum_{\langle ij\rangle} n_i n_j, \tag{7}$$

where $n_i = f^\dagger_{i\alpha} f_{i\alpha}$ and we assume the summation over the repeated indices unless explicitly mentioned. We note that the spinon description manifestly enlarges the physical Hilbert space. To remain in the physical Hilbert space, we utilize the half-filling constraint per site as $\sum_\alpha f^\dagger_{i\alpha} f_{i\alpha} = 1$. However, in this work, we assume this constraint to be loosely applicable in an average way in the spirit of mean field theory. Next, we perform only particle-hole mean-field decomposition to rewrite the Hamiltonian in Eq. (7) as

$$\mathcal{H}_{\text{heisen}} = -\frac{\tilde{J}}{2}\sum_{\langle ij\rangle}\left(m_{ji}f^\dagger_{i\alpha}f_{j\alpha} + \text{h.c.}\right) + \frac{\tilde{J}}{2}\sum_{\langle ij\rangle}|m_{ij}|^2, \tag{8}$$

where we have ignored the last term in Eq. (7), and introduced a mean-field ansatz as $m_{ij} = \langle f^\dagger_{i\alpha}f_{j\alpha}\rangle$. Similarly, we rewrite the chiral term as [7]

$$\begin{aligned}
\mathcal{H}_{\text{chiral}} &= \tilde{J}_\chi \sum_{\langle\langle ijk\rangle\rangle} \mathbf{S}_i\cdot(\mathbf{S}_j\times\mathbf{S}_k)\\
&= \frac{J_\chi}{8}\sum_{\langle\langle ijk\rangle\rangle}\left(f^\dagger_{i\alpha}\boldsymbol{\sigma}_{\alpha\beta}f_{i\beta}\right)\cdot\left(f^\dagger_{j\alpha'}\boldsymbol{\sigma}_{\alpha'\beta'}f_{j\beta'}\right)\times\left(f^\dagger_{k\alpha''}\boldsymbol{\sigma}_{\alpha''\beta''}f_{k\beta''}\right)\\
&= \frac{J_\chi}{8}\sum_{\langle\langle ijk\rangle\rangle}\epsilon_{abc}(\sigma^a)_{\alpha\beta}(\sigma^b)_{\alpha'\beta'}(\sigma^c)_{\alpha''\beta''}f^\dagger_{i\alpha}f_{i\beta}f^\dagger_{j\alpha'}f_{j\beta'}f^\dagger_{k\alpha''}f_{k\beta''}\\
&\approx \frac{3i\tilde{J}_\chi}{16}\sum_{\langle\langle ijk\rangle\rangle}\left(-m_{ik}m_{kj}m_{ji} + m_{kj}m_{ji}f^\dagger_{i\alpha}f_{k\alpha} + m_{ik}m_{kj}f^\dagger_{j\alpha}f_{i\alpha} + m_{ji}m_{ik}f^\dagger_{k\alpha}f_{j\alpha} - \text{h.c.}\right),
\end{aligned} \tag{9}$$

The total Hamiltonian is then $\mathcal{H}_{\text{pheno}} = \mathcal{H}_{\text{heisen}} + \mathcal{H}_{\text{chiral}}$. Without going into a self-consistent mean-field analysis, we assume a particular form of the mean fields and benchmark our analysis with our unbiased DMRG calculations. Assuming translational invariance, we choose $m_{ij} = m_0 e^{i\phi_{ij}}$, where m_0 is the amplitude of the order parameter and ϕ_{ij} are the bond-dependent phases. Now ignoring the amplitude and phase fluctuations, we can write the Hamiltonian as

$$\mathcal{H}_{\text{pheno}} = -\frac{\tilde{J}m_0}{2}\sum_{\langle ij\rangle}e^{i\phi_{ji}}f^\dagger_{i\alpha}f_{j\alpha} + \frac{3i\tilde{J}_\chi m_0^2}{16}\sum_{\langle ij\rangle}e^{i(\phi_{ik}+\phi_{kj})}f^\dagger_{j\alpha}f_{i\alpha} + \{i\leftrightarrow j\leftrightarrow k\} + 3\tilde{J}\sum_i m_0^2 + \frac{9\tilde{J}_\chi}{8}\sum_i m_0^3\cos\theta + \text{h.c} \tag{10}$$

Combining the hopping phases ϕ_{ij}'s, the above Hamiltonian can be written in a compact form as $\mathcal{H}_{\text{pheno}} = -\tilde{t}\sum_{\langle ij\rangle}e^{i\psi_{ij}}f^\dagger_{i\alpha}f_{j\alpha} + \text{h.c.}$, where $\tilde{t}$ is the spinon hopping amplitude and is related to our phenomenological parameters as

$$\tilde{t}\cos\psi_{ij} = \frac{\tilde{J}m_0}{2}\cos\phi_{ji} + \frac{3\tilde{J}_\chi m_0^2}{16}\sin\left(\phi_{ik}+\phi_{kj}\right), \tag{11a}$$

$$\tilde{t}\sin\psi_{ij} = \frac{\tilde{J}m_0}{2}\sin\phi_{ji} + \frac{3\tilde{J}_\chi m_0^2}{16}\cos\left(\phi_{ik}+\phi_{kj}\right), \tag{11b}$$

where $\psi_{ij} + \psi_{jk} + \psi_{ki} = \Phi_0$ with Φ_0 being total flux enclosed within a single triangular plaquette. At this point, all ϕ_{ij}/ψ_{ij} remains undetermined. Now we utilize Lieb's theorem [8] to determine the phases. According to the theorem, a fermion hopping on a bipartite lattice realizes the ground state with π-flux square plaquettes. Consequently, we consider a doubled unit cell such that one up and one down triangle jointly form the rhombus-like bipartite unit cell as shown in Fig. 1(a), and impose a π-flux in the doubled unit cell. This still leaves us with various choices for the bond-dependent phases ψ_{ij}, ψ_{jk}, and ψ_{ki} forming the triangular plaquette $\langle ijk\rangle$. A generic choice of the bond-dependent phases is shown in Fig. 1(a), where θ is some arbitrary angle specifying whether both the up and down triangles have the same flux $\pi/2$ or some staggered flux configurations as $\pi/2\pm\theta$ (both adding to π in the rhombus-shaped unit cell).

A. Topological spinon bands

We now move on to compute the spinon bands within the phenomenological flux phases in the triangle lattice. First of all, the primitive and the reciprocal lattice vectors of the original triangular lattice are given by

$$\mathbf{a}_1 = a\,(1,\ 0)\,,\ \ \mathbf{a}_2 = \frac{a}{2}\left(1,\ \sqrt{3}\right), \qquad \mathbf{b}_1 = \frac{2\pi}{\sqrt{3}a}\left(\sqrt{3},\ -1\right),\ \ \mathbf{b}_2 = \frac{4\pi}{\sqrt{3}a}\,(0,\ 1)\,, \tag{12}$$

where a is the lattice constant. The corresponding nearest-neighbor vectors as given by

$$\boldsymbol{\delta}_1 = a\,(1,\ 0)\,,\quad \boldsymbol{\delta}_2 = \frac{a}{2}\left(1,\ \sqrt{3}\right),\quad \boldsymbol{\delta}_3 = \frac{a}{2}\left(1,\ -\sqrt{3}\right). \tag{13}$$

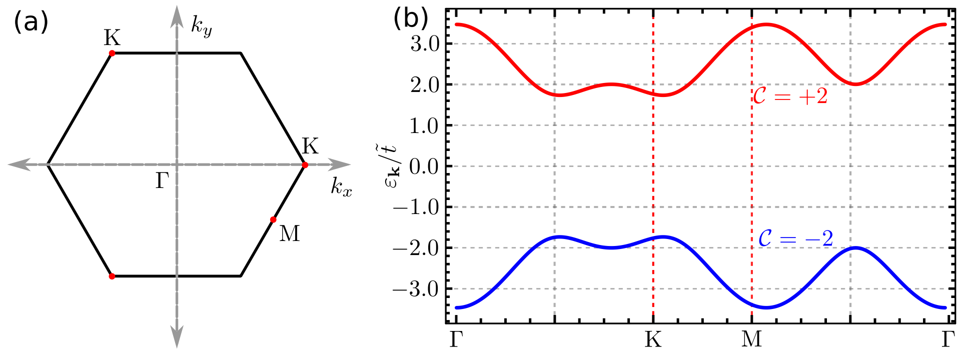

FIG. S1. (a) The Brillouin zone of a triangular lattice with the high-symmetry points marked by the filled circles. (b) The spectrum of gapped spinons within our mean-field approximation with the staggered phase $\theta = 0$. The topological Chern numbers are labeled on the two bands. Each spinon band is doubly degenerate in the spin degrees of freedom.

We also show the corresponding Brillouin zone (BZ) in Fig. S1(a) with the high-symmetry points as

$$\Gamma = (0,\ 0), \quad \mathrm{K} = \frac{\pi}{a}\left(\frac{4}{3},\ 0\right), \quad \mathrm{M} = \frac{\pi}{a}\left(1,\ \frac{1}{\sqrt{3}}\right). \tag{14}$$

Since the previous flux configuration doubles the unit cell as $\mathbf{a}_1 \to 2\mathbf{a}_1$, the tight-binding Hamiltonian in the sub-lattice basis (see Fig. 1(a) in the main text) is written as (note that we consider the uniform flux configuration with $\theta = 0$)

$$\mathcal{H}_{\mathrm{eff}} = -\tilde{t}\sum_i \left(f^\dagger_{i\mathrm{A}} f_{i+\boldsymbol{\delta}_1\mathrm{B}} + f^\dagger_{i\mathrm{A}} f_{i+\boldsymbol{\delta}_2\mathrm{A}} + i f^\dagger_{i\mathrm{A}} f_{i+\boldsymbol{\delta}_3\mathrm{B}} + f^\dagger_{i\mathrm{B}} f_{i+\boldsymbol{\delta}_1\mathrm{A}} - f^\dagger_{i\mathrm{B}} f_{i+\boldsymbol{\delta}_2\mathrm{B}} - i f^\dagger_{i\mathrm{B}} f_{i+\boldsymbol{\delta}_3\mathrm{A}}\right) + \mathrm{h.c.}, \tag{15}$$

Translating into the momentum space, we obtain

$$\mathcal{H}_{\mathrm{eff}} = -2\tilde{t}\sum_{\mathbf{k}} \begin{pmatrix} f^\dagger_{\mathbf{k}\mathrm{A}} & f^\dagger_{\mathbf{k}\mathrm{B}} \end{pmatrix} \begin{pmatrix} \cos\mathbf{k}\cdot\boldsymbol{\delta}_2 & \cos\mathbf{k}\cdot\boldsymbol{\delta}_1 + i\cos\mathbf{k}\cdot\boldsymbol{\delta}_3 \\ \cos\mathbf{k}\cdot\boldsymbol{\delta}_1 - i\cos\mathbf{k}\cdot\boldsymbol{\delta}_3 & -\cos\mathbf{k}\cdot\boldsymbol{\delta}_2 \end{pmatrix} \begin{pmatrix} f_{\mathbf{k}\mathrm{A}} \\ f_{\mathbf{k}\mathrm{B}} \end{pmatrix}. \tag{16}$$

The above Hamiltonian can be written in a compact form with Pauli matrices as $\mathcal{H}_{\mathrm{eff}} = -2t\sum_{\mathbf{k}} \mathbf{d}_{\mathbf{k}}\cdot\boldsymbol{\sigma}$ where

$$d_{1\mathbf{k}} = \cos\mathbf{k}\cdot\boldsymbol{\delta}_2, \quad d_{2\mathbf{k}} = \cos\mathbf{k}\cdot\boldsymbol{\delta}_1, \quad d_{3\mathbf{k}} = \cos\mathbf{k}\cdot\boldsymbol{\delta}_3. \tag{17}$$

The gapped spinon spectrum is obtained by diagonalizing the Hamiltonian in Eq. (16). The dispersion is given by $\varepsilon_{\mathbf{k}} = \pm 2\tilde{t}\sqrt{d^2_{1\mathbf{k}} + d^2_{2\mathbf{k}} + d^2_{3\mathbf{k}}}$ (see Fig. 1(b) in the main text). The spectrum remains gapped for any other choice of θ, except at $\theta = \frac{\pi}{2}$ when the gap closes as depicted in Fig. 1(c) in the main text. We computed the Chern number in the gapped phase using link variable method [9], and find the Chern numbers for the bands to be ± 2 (upon adding the spin degenerate bands) [see Fig. S1(b)].

B. Orbital electrical current and charge fluctuation in the gapped phase

In this section, we first provide the steps leading to an emergent non-vanishing loop electrical current distribution in the CSL phase. The current operator in the single-band Hubbard model reads as [10]

$$\hat{\boldsymbol{\mathcal{I}}}_{ij,k} = \hat{\mathbf{r}}_{ij}\frac{24e}{\hbar}\frac{t^3}{U^2}\mathbf{S}_k\cdot(\mathbf{S}_i \times \mathbf{S}_j)\,, \tag{18}$$

where $\hat{\mathbf{r}}_{ij}$ is the unit vector connecting two sites i, j, and the localized current flows within a triangular loop. Rewriting in terms of the spinons, we obtain

$$\begin{aligned} \hat{\boldsymbol{\mathcal{I}}}_{ij,k} =& \hat{\mathbf{r}}_{ij}\frac{e}{\hbar}\frac{9it^3}{2U^2}\left(m_{kj}m_{ji}f^\dagger_{i\alpha}f_{k\alpha} + m_{ik}m_{kj}f^\dagger_{j\alpha}f_{i\alpha} + m_{ji}m_{ik}f^\dagger_{k\alpha}f_{j\alpha} - \mathrm{h.c.}\right) \\ =& \hat{\mathbf{r}}_{ij}\frac{9im_0^2t^3}{U^2}e^{i(\phi_{ik}+\phi_{kj})}f^\dagger_j f_i + \underbrace{k\to j\to i}_{} + \underbrace{j\to i\to k}_{} + \mathrm{h.c.} \end{aligned} \tag{19}$$

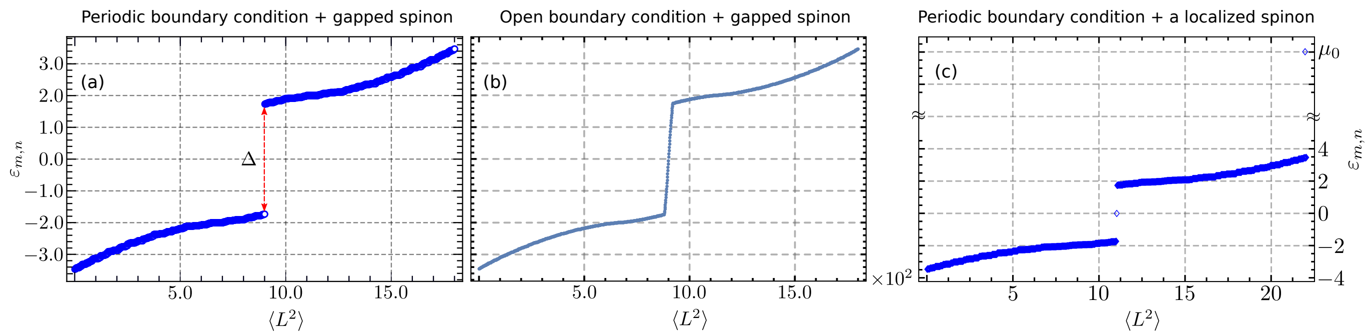

FIG. S2. (a) The eigenvalue distribution of the real-space Hamiltonian (PBC) as a function of the system size. The topological protection manifests into a gap in the eigenvalue distribution. (b) The eigenvalue distribution of the real-space Hamiltonian as a function of the system size in open boundary conditions with the edge modes in the gap. (c) The eigenvalue distribution of the real-space Hamiltonian as a function of the system size for the triangular lattice in periodic boundary conditions. We set a local chemical potential V_0 at site $\mathbf{r}_0$ for the A-sublattice. For very large V_0, there are two additional states which are shown by the symbols around zero energy and the other one at higher energy dictated by V_0.

Note that in the last line, we removed the spin-label. Since the spinon bands are degenerate in the spin degrees of freedom, we have added the contributions from both spin channels. In a similar spirit, we can re-express the charge fluctuation operator in spinon language as [10]

$$\delta\rho_{i,jk} = e\frac{8t^3}{U^3}\left(\mathbf{S}_i\cdot\mathbf{S}_j + \mathbf{S}_i\cdot\mathbf{S}_k - 2\mathbf{S}_j\cdot\mathbf{S}_k\right) = e\frac{8m_0t^3}{U^3}\left(e^{i\phi_{ji}}f_i^\dagger f_j + e^{i\phi_{ki}}f_i^\dagger f_k - 2e^{i\phi_{kj}}f_j^\dagger f_k\right) + \text{h.c.}, \tag{20}$$

where we again added the spin degeneracy in the last line of the above equation.

As we are interested in the real space loop current and chare fluctuation profile, we consider a real-space calculation to evaluate the loop current expectation values. The Hamiltonian in Eq. (16) is therefore written on a 2D triangle lattice of size $L\times L$ unit cells. Since each unit cell contains two sub-lattice sites (A & B), there are $2L^2$ spinon operators $f_{i\sigma}^\dagger$ in the system. The lattice vectors are chosen as $\mathbf{a}_1 = (2,0)$, and $\mathbf{a}_2 = (1/2, \sqrt{3}/2)$. The spinon operators at a site i is written as $f_i^\dagger = f_\eta^\dagger(m,n)$, where η corresponds to the sub-lattice index, and $\mathbf{R}(m,n) = m\mathbf{a}_1 + n\mathbf{a}_2$, $m,n = 1,2,\dots L$. If we impose periodic boundary condition (PBC), then the spinon operators follow $f_\eta^\dagger(m+L,n) = f_\eta^\dagger(m,n)$, and $f_\eta^\dagger(m,n+L) = f_\eta^\dagger(m,n)$, otherwise $f_\eta^\dagger(m+L,n) = f_\eta^\dagger(m,n+L) = 0$ in the open boundary condition (OBC). The $2L^2$-dimensional spinon vector is constructed as $\tilde{\mathbf{f}}^\dagger = (f_{\mathrm{A}}^\dagger, f_{\mathrm{B}}^\dagger)$ with

$$f_\eta^\dagger = \left(f_\eta^\dagger(1,1), f_\eta^\dagger(2,1), \dots f_\eta^\dagger(L,1), f_\eta^\dagger(1,2), f_\eta^\dagger(2,2), \dots f_\eta^\dagger(L,2), \dots, f_\eta^\dagger(L,L)\right), \quad \eta\in\{\mathrm{A},\mathrm{B}\}. \tag{21}$$

In terms of the spinon vector $\tilde{\mathbf{f}}^\dagger$, we can write the the Hamiltonian in Eq. (16) as $\mathcal{H}_{\text{eff}} = \tilde{\mathbf{f}}^\dagger \mathsf{H}\tilde{\mathbf{f}}$, where H is written as a $2L^2\times 2L^2$ matrix. On the diagonal basis, we can rewrite the spinon operators as

$$\begin{bmatrix}\zeta_{u\sigma}(m,n)\\ \zeta_{d\sigma}(m,n)\end{bmatrix} = \sum_{m,n} \mathrm{U}_{mn}\cdot\begin{bmatrix}f_{\mathrm{A}\sigma}(m,n)\\ f_{\mathrm{B}\sigma}(m,n)\end{bmatrix}, \tag{22}$$

where U is the diagonalizing matrix for Hamiltonian H, and $\zeta_{u/d}(m,n)$ are the diagonal spinon operators corresponding to the spectrum as shown in Fig. S2. In panel (a), we show the band dispersion with a topological gap Δ in the PBC, while in panel (b), the spectrum in the case of OBC is shown with an edge mode inside the bulk gap Δ. The spectrum for a localized spinon at site $\mathbf{r}_0$ inside the bulk is shown in panel (c). To realize the latter scenario, we impose a large onsite chemical potential V_0 at the site $\mathbf{r}_0$ within the unit cell. Due to the large energy, this specific site will not host any spinons and can be thought of as a localized spinon hole. The physical situation might be some empty defect sites, or some magnetic impurity sitting inside the bulk of the system.

Analysis of the expectation values

Once we know all the eigenenergy and the eigenstates of the Hamiltonian, it is straightforward to obtain the average of the loop current operator in the ground state. The target quantity of our interest is $\langle f_\alpha^\dagger(\mathbf{R}_{mn}) f_\beta(\mathbf{R}'_{m'n'})\rangle$ for $\{\alpha,\beta\}\in\{\mathrm{A},\mathrm{B}\}$, where $\mathbf{R}_{mn}$ denotes the position of the site at $\mathbf{R}_{mn} = m\hat{\mathbf{a}}_1 + n\hat{\mathbf{a}}_2$. The analysis goes as follows

$$\langle f_\alpha^\dagger(\mathbf{R}_{mn}) f_\beta(\mathbf{R}'_{m'n'})\rangle = \left\langle \begin{pmatrix} f_{\mathrm{A}}^\dagger & f_{\mathrm{B}}^\dagger\end{pmatrix} \mathcal{W}^{(\alpha\beta)}_{\mathbf{R}\mathbf{R}'} \begin{pmatrix} f_{\mathrm{A}}\\ f_{\mathrm{B}}\end{pmatrix}\right\rangle = \sum_{ll'=1}^{2L^2}\left(U^\dagger \mathcal{W}^{(\alpha\beta)}_{\mathbf{R}\mathbf{R}'} U\right)_{ll'} \langle \zeta_l^\dagger \zeta_{l'}\rangle = \sum_{l=L^2+1}^{2L^2}\left(U^\dagger \mathcal{W}^{(\alpha\beta)}_{\mathbf{R}\mathbf{R}'} U\right)_{ll}, \tag{23}$$

where $\langle \zeta_l^\dagger \zeta_{l'} \rangle = \delta_{ll'}$, and the $2L^2 \times 2L^2$ matrices $\mathcal{W}^{(\alpha\beta)}_{\mathbf{RR'}}$ are defined as follows

$$\mathcal{W}^{(\alpha\beta)}_{\mathbf{RR'}} = \begin{pmatrix} \mathcal{B}^{\mathrm{AA}}_{\mathbf{RR'}}\delta_{\alpha\mathrm{A}}\delta_{\beta\mathrm{A}} & \mathcal{B}^{\mathrm{AB}}_{\mathbf{RR'}}\delta_{\alpha\mathrm{A}}\delta_{\beta\mathrm{B}} \\ \mathcal{B}^{\mathrm{BA}}_{\mathbf{RR'}}\delta_{\alpha\mathrm{B}}\delta_{\beta\mathrm{A}} & \mathcal{B}^{\mathrm{BB}}_{\mathbf{RR'}}\delta_{\alpha\mathrm{B}}\delta_{\beta\mathrm{B}} \end{pmatrix}. \tag{24}$$

Here, $\mathcal{B}^{(\alpha)}_{\mathbf{RR'}}$ are $L^2 \times L^2$ matrices corresponding to the non-zero connections allowed by the orientations of the triangles. The corresponding results for the charge fluctuation and loop current distribution are shown in Fig. 3(a-c) in the main text.

III. DYNAMIC SPIN STRUCTURE FACTOR

In this section, we provide the details of the analysis of the dynamical spin structure factor (DSSF). The latter is defined as

$$S(\mathbf{q},\omega) = \sum_{i,j} \frac{e^{i\mathbf{q}\cdot(\mathbf{r}_i - \mathbf{r}_j)}}{N_s} \int_{-\infty}^{\infty} dt e^{i\omega t} \langle \mathbf{S}_i(t) \cdot \mathbf{S}_j(0) \rangle , \tag{25}$$

where i,j corresponds to the position of the unit cell containing two sub-lattice sites. Note that the unit-cell i has two sub-lattice sites labeled by A, and B. Consequently, we can rewrite the above equation as

$$\begin{aligned} S(\mathbf{q},\omega) = \sum_{i,j} \frac{e^{i\mathbf{q}\cdot(\mathbf{r}_i - \mathbf{r}_j)}}{N_s} \int_{-\infty}^{\infty} dt e^{i\omega t} \Big[& \langle \mathbf{S}_{i,\mathrm{A}}(t) \cdot \mathbf{S}_{j,\mathrm{A}}(0) \rangle + \langle \mathbf{S}_{i,\mathrm{B}}(t) \cdot \mathbf{S}_{j,\mathrm{B}}(0) \rangle + \\ & e^{i\mathbf{q}\cdot\mathbf{a_1}} \langle \mathbf{S}_{i,\mathrm{A}}(t) \cdot \mathbf{S}_{j,\mathrm{B}}(0) \rangle + e^{-i\mathbf{q}\cdot\mathbf{a_1}} \langle \mathbf{S}_{i,\mathrm{B}}(t) \cdot \mathbf{S}_{j,\mathrm{A}}(0) \rangle \Big], \end{aligned} \tag{26}$$

where we have explicitly written down the DSSF in sub-lattice resolved coordinates. It is straightforward to show next that a typical sub-lattice resolved term is given by ($\{\eta,\zeta\} \in \{\mathrm{A},\mathrm{B}\}$)

$$\begin{aligned} S^{\eta\zeta}(\mathbf{q},\omega) &= \sum_{i,j} \frac{e^{i\mathbf{q}\cdot(\mathbf{r}_i - \mathbf{r}_j)}}{4N_s} \int_{-\infty}^{\infty} dt e^{i\omega t} e^{i(E_0 - E_n)t} \langle 0 | f^\dagger_{i\eta\alpha} f_{i\eta\beta} | n \rangle \langle n | f^\dagger_{j\zeta\gamma} f_{j\zeta\delta} | 0 \rangle \left(2\delta_{\alpha\delta}\delta_{\beta\gamma} - \delta_{\alpha\beta}\delta_{\gamma\delta}\right) \\ &= \sum_{\mathbf{k},\mathbf{p}} \sum_n \frac{2\delta_{\alpha\delta}\delta_{\beta\gamma} - \delta_{\alpha\beta}\delta_{\gamma\delta}}{4} \delta(\omega - E_n + E_0) \langle 0 | f^\dagger_{\mathbf{p}\eta\alpha} f_{\mathbf{p}+\mathbf{q}\eta\beta} | n \rangle \langle n | f^\dagger_{\mathbf{k}+\mathbf{q}\zeta\gamma} f_{\mathbf{k}\zeta\delta} | 0 \rangle \\ &= \sum_{\mathbf{k}} \sum_n \frac{2\delta_{\alpha\delta}\delta_{\beta\gamma} - \delta_{\alpha\beta}\delta_{\gamma\delta}}{4} \delta(\omega - E_n + E_0) \langle 0 | f^\dagger_{\mathbf{k}\eta\alpha} f_{\mathbf{k}+\mathbf{q}\eta\beta} | n \rangle \langle n | f^\dagger_{\mathbf{k}+\mathbf{q}\zeta\gamma} f_{\mathbf{k}\zeta\delta} | 0 \rangle \\ &= \sum_{\mathbf{k}} \sum_n \delta(\omega - E_n + E_0) \left(\frac{\langle 0 | f^\dagger_{\mathbf{k}\eta\alpha} f_{\mathbf{k}+\mathbf{q}\eta\beta} | n \rangle \langle n | f^\dagger_{\mathbf{k}+\mathbf{q}\zeta\beta} f_{\mathbf{k}\zeta\alpha} | 0 \rangle}{2} - \frac{\langle 0 | f^\dagger_{\mathbf{k}\eta\alpha} f_{\mathbf{k}+\mathbf{q}\eta\alpha} | n \rangle \langle n | f^\dagger_{\mathbf{k}+\mathbf{q}\zeta\beta} f_{\mathbf{k}\zeta\beta} | 0 \rangle}{4} \right) \\ &= \sum_{\mathbf{k}} \sum_n \delta(\omega - E_n + E_0) \left(\frac{\langle 0 | f^\dagger_{\mathbf{k}\eta\alpha} f_{\mathbf{k}+\mathbf{q}\eta\beta} | n \rangle \langle n | f^\dagger_{\mathbf{k}+\mathbf{q}\zeta\beta} f_{\mathbf{k}\zeta\alpha} | 0 \rangle}{2} - \frac{\langle 0 | f^\dagger_{\mathbf{k}\eta\alpha} f_{\mathbf{k}+\mathbf{q}\eta\alpha} | n \rangle \langle n | f^\dagger_{\mathbf{k}+\mathbf{q}\zeta\alpha} f_{\mathbf{k}\zeta\alpha} | 0 \rangle}{4} \right) \\ &= \frac{3}{2} \sum_{\mathbf{k}} \sum_n \delta(\omega - E_n + E_0) \langle 0 | f^\dagger_{\mathbf{k}\eta} f_{\mathbf{k}+\mathbf{q}\eta} | n \rangle \langle n | f^\dagger_{\mathbf{k}+\mathbf{q}\zeta} f_{\mathbf{k}\zeta} | 0 \rangle , \end{aligned} \tag{27}$$

where in the last line, we have summed over the degenerate spin degrees of freedom and omitted the spin indices, and $|n\rangle$ corresponds to an excited eigenmode with energy E_n. We perform the numerical integration in Mathematica and the corresponding plots are shown in Fig. 4 in the main text. We approximate the delta function $\delta(x)$ as $\delta(x) = \frac{1}{\pi}\frac{\gamma^2}{x^2+\gamma^2}$, and considered $\gamma = 0.1$ for numerical purposes.

IV. OPTICAL CONDUCTIVITY IN THE CSL PHASE

Finally, in this section, we provide the details of the analysis for the transverse and longitudinal optical conductivity in the CSL phase. Since the parent compound is a Mott insulator, we do not have any mobile charges; however, the

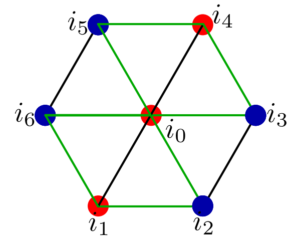

FIG. S3. Contribution to the polarization from a single site at i_0 surrounded by six triangles with sites $i_1, \ldots, i_6$.

charge fluctuations in the insulating phase will lead to electrical polarization which couples to the external electric field and lead to finite optical conductivity. The corresponding electrical susceptibility is given by

$$\chi_{xy}(\omega) = -\frac{V}{\hbar}\sum_{n\neq 0}\left[\frac{\langle\psi_0|P_x|\psi_n\rangle\langle\psi_n|P_y|\psi_0\rangle}{\omega-\omega_n+i\eta} - \frac{\langle\psi_0|P_y|\psi_n\rangle\langle\psi_n|P_x|\psi_0\rangle}{\omega+\omega_n+i\eta}\right], \tag{28}$$

where $\mathbf{P} = P_x\hat{\mathbf{x}} + P_y\hat{\mathbf{y}}$ is the total polarization in the system. For a triangular plaquette, the corresponding expression can be obtained from the charge fluctuation operators [10]. Here, we consider a single site at i_0 embedded in the lattice as shown in Fig. S3. The polarization for each triangle is thereafter written as

$$\mathbf{P}_{i_0;i_1i_2} = -\frac{12eat^3}{U^3}\left(\mathbf{S}_{i_0}\cdot\mathbf{S}_{i_1} - \mathbf{S}_{i_0}\cdot\mathbf{S}_{i_2}\right)\hat{\mathbf{x}} + \frac{4\sqrt{3}eat_{\text{hop}}^3}{U^3}\left(\mathbf{S}_{i_0}\cdot\mathbf{S}_{i_1} + \mathbf{S}_{i_0}\cdot\mathbf{S}_{i_2} - 2\mathbf{S}_{i_1}\cdot\mathbf{S}_{i_2}\right)\hat{\mathbf{y}}, \tag{29a}$$

$$\mathbf{P}_{i_0;i_4i_5} = \frac{12eat^3}{U^3}\left(\mathbf{S}_{i_0}\cdot\mathbf{S}_{i_4} - \mathbf{S}_{i_0}\cdot\mathbf{S}_{i_5}\right)\hat{\mathbf{x}} - \frac{4\sqrt{3}eat_{\text{hop}}^3}{U^3}\left(\mathbf{S}_{i_0}\cdot\mathbf{S}_{i_4} + \mathbf{S}_{i_0}\cdot\mathbf{S}_{i_5} - 2\mathbf{S}_{i_4}\cdot\mathbf{S}_{i_5}\right)\hat{\mathbf{y}}, \tag{29b}$$

$$\mathbf{P}_{i_0;i_2i_3} = \frac{12eat^3}{U^3}\left(\mathbf{S}_{i_2}\cdot\mathbf{S}_{i_3} - \mathbf{S}_{i_0}\cdot\mathbf{S}_{i_2}\right)\hat{\mathbf{x}} - \frac{4\sqrt{3}eat_{\text{hop}}^3}{U^3}\left(\mathbf{S}_{i_0}\cdot\mathbf{S}_{i_2} + \mathbf{S}_{i_2}\cdot\mathbf{S}_{i_3} - 2\mathbf{S}_{i_0}\cdot\mathbf{S}_{i_3}\right)\hat{\mathbf{y}}, \tag{29c}$$

$$\mathbf{P}_{i_0;i_5i_6} = -\frac{12eat^3}{U^3}\left(\mathbf{S}_{i_5}\cdot\mathbf{S}_{i_6} - \mathbf{S}_{i_0}\cdot\mathbf{S}_{i_5}\right)\hat{\mathbf{x}} + \frac{4\sqrt{3}eat_{\text{hop}}^3}{U^3}\left(\mathbf{S}_{i_0}\cdot\mathbf{S}_{i_5} + \mathbf{S}_{i_5}\cdot\mathbf{S}_{i_6} - 2\mathbf{S}_{i_0}\cdot\mathbf{S}_{i_6}\right)\hat{\mathbf{y}}, \tag{29d}$$

$$\mathbf{P}_{i_0;i_3i_4} = \frac{12eat^3}{U^3}\left(\mathbf{S}_{i_3}\cdot\mathbf{S}_{i_4} - \mathbf{S}_{i_0}\cdot\mathbf{S}_{i_4}\right)\hat{\mathbf{x}} + \frac{4\sqrt{3}eat_{\text{hop}}^3}{U^3}\left(\mathbf{S}_{i_0}\cdot\mathbf{S}_{i_4} + \mathbf{S}_{i_3}\cdot\mathbf{S}_{i_4} - 2\mathbf{S}_{i_0}\cdot\mathbf{S}_{i_3}\right)\hat{\mathbf{y}}, \tag{29e}$$

$$\mathbf{P}_{i_0;i_6i_1} = -\frac{12eat^3}{U^3}\left(\mathbf{S}_{i_6}\cdot\mathbf{S}_{i_1} - \mathbf{S}_{i_0}\cdot\mathbf{S}_{i_1}\right)\hat{\mathbf{x}} - \frac{4\sqrt{3}eat_{\text{hop}}^3}{U^3}\left(\mathbf{S}_{i_0}\cdot\mathbf{S}_{i_1} + \mathbf{S}_{i_6}\cdot\mathbf{S}_{i_1} - 2\mathbf{S}_{i_0}\cdot\mathbf{S}_{i_6}\right)\hat{\mathbf{y}}. \tag{29f}$$

Now, we can add all these contributions to obtain the total polarization per site i_0 as

$$\begin{aligned}\mathbf{P}_{i_0} &= \frac{12eat^3}{U^3}\left(\mathbf{S}_{i_2}\cdot\mathbf{S}_{i_3} - \mathbf{S}_{i_5}\cdot\mathbf{S}_{i_6} + \mathbf{S}_{i_3}\cdot\mathbf{S}_{i_4} - \mathbf{S}_{i_6}\cdot\mathbf{S}_{i_1}\right)\hat{\mathbf{x}} \\ &\quad - \frac{4\sqrt{3}eat^3}{U^3}\left(2\mathbf{S}_{i_1}\cdot\mathbf{S}_{i_2} + \mathbf{S}_{i_2}\cdot\mathbf{S}_{i_3} - \mathbf{S}_{i_3}\cdot\mathbf{S}_{i_4} - 2\mathbf{S}_{i_4}\cdot\mathbf{S}_{i_5} - \mathbf{S}_{i_5}\cdot\mathbf{S}_{i_6} + \mathbf{S}_{i_6}\cdot\mathbf{S}_{i_1}\right)\hat{\mathbf{y}}.\end{aligned} \tag{30}$$

We further utlize the Pauli matrix identities and rewrite the above expression in the spinon language as

$$\begin{aligned}\mathbf{P}_{i_0} = \frac{3eat^3}{U^3}\delta_{\alpha\beta\gamma\delta}&\left(f^\dagger_{i_2\alpha}f^\dagger_{i_3\gamma}f_{i_3\delta}f_{i_2\beta} - f^\dagger_{i_5\alpha}f^\dagger_{i_6\gamma}f_{i_6\delta}f_{i_5\beta} + f^\dagger_{i_3\alpha}f^\dagger_{i_4\gamma}f_{i_4\delta}f_{i_3\beta} - f^\dagger_{i_6\alpha}f^\dagger_{i_1\gamma}f_{i_1\delta}f_{i_6\beta}\right)\hat{\mathbf{x}} - \frac{\sqrt{3}eat^3}{U^3}\delta_{\alpha\beta\gamma\delta}\left(2f^\dagger_{i_1\alpha}f^\dagger_{i_2\gamma}f_{i_2\delta}f_{i_1\beta}\right. \\ &\left.+f^\dagger_{i_2\alpha}f^\dagger_{i_3\gamma}f_{i_3\delta}f_{i_2\beta} - f^\dagger_{i_3\alpha}f^\dagger_{i_4\gamma}f_{i_4\delta}f_{i_3\beta} - 2f^\dagger_{i_4\alpha}f^\dagger_{i_5\gamma}f_{i_5\delta}f_{i_4\beta} - f^\dagger_{i_5\alpha}f^\dagger_{i_6\gamma}f_{i_6\delta}f_{i_5\beta} + f^\dagger_{i_6\alpha}f^\dagger_{i_1\gamma}f_{i_1\delta}f_{i_6\beta}\right)\hat{\mathbf{y}},\end{aligned} \tag{31}$$

where $\delta_{\alpha\beta\gamma\delta} = 2\delta_{\alpha\delta}\delta_{\beta\gamma} - \delta_{\alpha\beta}\delta_{\gamma\delta}$. Consequently, we can obtain the total polarization which is the sum over two sub-lattice polarizations as

$$\mathbf{P} = \frac{1}{V}\left(\sum_{i_0\in\text{A}}\mathbf{P}_{i_0} + \sum_{i_0\in\text{B}}\mathbf{P}_{i_0}\right). \tag{32}$$

Rewriting it in the momentum space we obtain in the sub-lattice basis as

$$P^x_{i_0\in\mathrm{A}} = \frac{3eat^3}{U^3}\sum_{\{\mathbf{k}\}}\delta_{\alpha\beta\gamma\delta}\Big(e^{i\mathbf{k}_1\cdot\mathbf{r}_2+i\mathbf{k}_2\cdot\mathbf{r}_3-i\mathbf{k}_3\cdot\mathbf{r}_3-i\mathbf{k}_4\cdot\mathbf{r}_2}f^\dagger_{\mathrm{B}\mathbf{k}_1\alpha}f^\dagger_{\mathrm{B}\mathbf{k}_2\gamma}f_{\mathrm{B}\mathbf{k}_3\delta}f_{\mathrm{B}\mathbf{k}_4\beta} - e^{i\mathbf{k}_1\cdot\mathbf{r}_5+i\mathbf{k}_2\cdot\mathbf{r}_6-i\mathbf{k}_3\cdot\mathbf{r}_6-i\mathbf{k}_4\cdot\mathbf{r}_5}f^\dagger_{\mathrm{B}\mathbf{k}_1\alpha}f^\dagger_{\mathrm{B}\mathbf{k}_2\gamma}f_{\mathrm{B}\mathbf{k}_3\delta}f_{\mathrm{B}\mathbf{k}_4\beta}$$
$$+e^{i\mathbf{k}_1\cdot\mathbf{r}_3+i\mathbf{k}_2\cdot\mathbf{r}_4-i\mathbf{k}_3\cdot\mathbf{r}_4-i\mathbf{k}_4\cdot\mathbf{r}_3}f^\dagger_{\mathrm{B}\mathbf{k}_1\alpha}f^\dagger_{\mathrm{A}\mathbf{k}_2\gamma}f_{\mathrm{A}\mathbf{k}_3\delta}f_{\mathrm{B}\mathbf{k}_4\beta} - e^{i\mathbf{k}_1\cdot\mathbf{r}_6+i\mathbf{k}_2\cdot\mathbf{r}_1-i\mathbf{k}_3\cdot\mathbf{r}_1-i\mathbf{k}_4\cdot\mathbf{r}_6}f^\dagger_{\mathrm{B}\mathbf{k}_1\alpha}f^\dagger_{\mathrm{A}\mathbf{k}_2\gamma}f_{\mathrm{A}\mathbf{k}_3\delta}f_{\mathrm{B}\mathbf{k}_4\beta}\Big), \quad (33a)$$

$$P^y_{i_0\in\mathrm{A}} = \frac{\sqrt{3}eat^3}{U^3}\sum_{\{\mathbf{k}\}}\delta_{\alpha\beta\gamma\delta}\Big(2e^{i\mathbf{k}_1\cdot\mathbf{r}_1+i\mathbf{k}_2\cdot\mathbf{r}_2-i\mathbf{k}_3\cdot\mathbf{r}_2-i\mathbf{k}_4\cdot\mathbf{r}_1}f^\dagger_{\mathrm{A}\mathbf{k}_1\alpha}f^\dagger_{\mathrm{B}\mathbf{k}_2\gamma}f_{\mathrm{B}\mathbf{k}_3\delta}f_{\mathrm{A}\mathbf{k}_4\beta} + e^{i\mathbf{k}_1\cdot\mathbf{r}_2+i\mathbf{k}_2\cdot\mathbf{r}_3-i\mathbf{k}_3\cdot\mathbf{r}_3-i\mathbf{k}_4\cdot\mathbf{r}_2}f^\dagger_{\mathrm{B}\mathbf{k}_1\alpha}f^\dagger_{\mathrm{B}\mathbf{k}_2\gamma}f_{\mathrm{B}\mathbf{k}_3\delta}f_{\mathrm{B}\mathbf{k}_4\beta}$$
$$-e^{i\mathbf{k}_1\cdot\mathbf{r}_3+i\mathbf{k}_2\cdot\mathbf{r}_4-i\mathbf{k}_3\cdot\mathbf{r}_4-i\mathbf{k}_4\cdot\mathbf{r}_3}f^\dagger_{\mathrm{B}\mathbf{k}_1\alpha}f^\dagger_{\mathrm{A}\mathbf{k}_2\gamma}f_{\mathrm{A}\mathbf{k}_3\alpha}f_{\mathrm{B}\mathbf{k}_4\beta} - 2e^{i\mathbf{k}_1\cdot\mathbf{r}_4+i\mathbf{k}_2\cdot\mathbf{r}_5-i\mathbf{k}_3\cdot\mathbf{r}_5-i\mathbf{k}_4\cdot\mathbf{r}_4}f^\dagger_{\mathrm{A}\mathbf{k}_1\alpha}f^\dagger_{\mathrm{B}\mathbf{k}_2\gamma}f_{\mathrm{B}\mathbf{k}_3\alpha}f_{\mathrm{A}\mathbf{k}_4\beta}$$
$$-e^{i\mathbf{k}_1\cdot\mathbf{r}_5+i\mathbf{k}_2\cdot\mathbf{r}_6-i\mathbf{k}_3\cdot\mathbf{r}_6-i\mathbf{k}_4\cdot\mathbf{r}_5}f^\dagger_{\mathrm{B}\mathbf{k}_1\alpha}f^\dagger_{\mathrm{B}\mathbf{k}_2\gamma}f_{\mathrm{B}\mathbf{k}_3\delta}f_{\mathrm{B}\mathbf{k}_4\beta} + e^{i\mathbf{k}_1\cdot\mathbf{r}_6+i\mathbf{k}_2\cdot\mathbf{r}_1-i\mathbf{k}_3\cdot\mathbf{r}_1-i\mathbf{k}_4\cdot\mathbf{r}_6}f^\dagger_{\mathrm{B}\mathbf{k}_1\alpha}f^\dagger_{\mathrm{A}\mathbf{k}_2\gamma}f_{\mathrm{A}\mathbf{k}_3\delta}f_{\mathrm{B}\mathbf{k}_4\beta}\Big), \quad (33b)$$

whereas for $i_0 \in \mathrm{B}$, we need to update the above expression with A $\leftrightarrow$ B. Now, we utilize the vector relation as $\mathbf{r}_i = \mathbf{r}_{i_0} + \mathbf{\Delta}_i, \forall i = 1,\ldots 6$, where $\mathbf{\Delta}_i$ is the nearest neighbor site to i_0, and they are related to the original nearest-neighbor vectors defined as

$$\mathbf{\Delta}_1 = -\boldsymbol{\delta}_2, \quad \mathbf{\Delta}_2 = \boldsymbol{\delta}_3, \quad \mathbf{\Delta}_3 = \boldsymbol{\delta}_1, \quad \mathbf{\Delta}_4 = \boldsymbol{\delta}_2, \quad \mathbf{\Delta}_5 = -\boldsymbol{\delta}_3, \quad \mathbf{\Delta}_6 = -\boldsymbol{\delta}_1. \quad (34)$$

Taking the summation over all the sites i_0, we have

$$\sum_{i_0} P^x_{i_0\in\mathrm{A}} = \frac{6ieat^3}{U^3}\sum_{\{\mathbf{k}\}}{}' \delta_{\alpha\beta\gamma\delta}\Big(\sin\left[\mathbf{k}_1\cdot\boldsymbol{\delta}_3 + \mathbf{k}_2\cdot\boldsymbol{\delta}_1 - \mathbf{k}_3\cdot\boldsymbol{\delta}_1 - \mathbf{k}_4\cdot\boldsymbol{\delta}_3\right]f^\dagger_{\mathrm{B}\mathbf{k}_1\alpha}f^\dagger_{\mathrm{B}\mathbf{k}_2\gamma}f_{\mathrm{B}\mathbf{k}_3\delta}f_{\mathrm{B}\mathbf{k}_4\beta} +$$
$$\sin\left[\mathbf{k}_1\cdot\boldsymbol{\delta}_1 + \mathbf{k}_2\cdot\boldsymbol{\delta}_2 - \mathbf{k}_3\cdot\boldsymbol{\delta}_2 - \mathbf{k}_4\cdot\boldsymbol{\delta}_1\right]f^\dagger_{\mathrm{B}\mathbf{k}_1\alpha}f^\dagger_{\mathrm{A}\mathbf{k}_2\gamma}f_{\mathrm{A}\mathbf{k}_3\delta}f_{\mathrm{B}\mathbf{k}_4\beta}\Big), \quad (35a)$$

$$\sum_{i_0} P^y_{i_0\in\mathrm{A}} = \frac{2\sqrt{3}ieat^3}{U^3}\sum_{\{\mathbf{k}\}}{}' \delta_{\alpha\beta\gamma\delta}\Big(2\sin[-\mathbf{k}_1\cdot\boldsymbol{\delta}_2 + \mathbf{k}_2\cdot\boldsymbol{\delta}_3 - \mathbf{k}_3\cdot\boldsymbol{\delta}_3 + \mathbf{k}_4\cdot\boldsymbol{\delta}_2]f^\dagger_{\mathrm{A}\mathbf{k}_1\alpha}f^\dagger_{\mathrm{B}\mathbf{k}_2\gamma}f_{\mathrm{B}\mathbf{k}_3\delta}f_{\mathrm{A}\mathbf{k}_4\beta} +$$
$$\sin[\mathbf{k}_1\cdot\boldsymbol{\delta}_3 + \mathbf{k}_2\cdot\boldsymbol{\delta}_1 - \mathbf{k}_3\cdot\boldsymbol{\delta}_1 - \mathbf{k}_4\cdot\boldsymbol{\delta}_3]f^\dagger_{\mathrm{B}\mathbf{k}_1\alpha}f^\dagger_{\mathrm{B}\mathbf{k}_2\gamma}f_{\mathrm{B}\mathbf{k}_3\delta}f_{\mathrm{B}\mathbf{k}_4\beta} -$$
$$\sin[\mathbf{k}_1\cdot\boldsymbol{\delta}_1 + \mathbf{k}_2\cdot\boldsymbol{\delta}_2 - \mathbf{k}_3\cdot\boldsymbol{\delta}_2 - \mathbf{k}_4\cdot\boldsymbol{\delta}_1]f^\dagger_{\mathrm{B}\mathbf{k}_1\alpha}f^\dagger_{\mathrm{A}\mathbf{k}_2\gamma}f_{\mathrm{A}\mathbf{k}_3\delta}f_{\mathrm{B}\mathbf{k}_4\beta}\Big), \quad (35b)$$

where $\sum'$ denotes the momentum conversation, *i.e.*, $\mathbf{k}_1 + \mathbf{k}_2 = \mathbf{k}_3 + \mathbf{k}_4$, obtained by summing over all the sites.

$$P^x = \frac{6ieat^3}{U^3}\sum_{\{\mathbf{k}\}}{}' \delta_{\alpha\beta\gamma\delta}\Big(\sin\left[\mathbf{k}_1\cdot\boldsymbol{\delta}_3 + \mathbf{k}_2\cdot\boldsymbol{\delta}_1 - \mathbf{k}_3\cdot\boldsymbol{\delta}_1 - \mathbf{k}_4\cdot\boldsymbol{\delta}_3\right](f^\dagger_{\mathrm{B}\mathbf{k}_1\alpha}f^\dagger_{\mathrm{B}\mathbf{k}_2\gamma}f_{\mathrm{B}\mathbf{k}_3\delta}f_{\mathrm{B}\mathbf{k}_4\beta} + f^\dagger_{\mathrm{A}\mathbf{k}_1\alpha}f^\dagger_{\mathrm{A}\mathbf{k}_2\gamma}f_{\mathrm{A}\mathbf{k}_3\delta}f_{\mathrm{A}\mathbf{k}_4\beta}) +$$
$$\sin\left[\mathbf{k}_1\cdot\boldsymbol{\delta}_1 + \mathbf{k}_2\cdot\boldsymbol{\delta}_2 - \mathbf{k}_3\cdot\boldsymbol{\delta}_2 - \mathbf{k}_4\cdot\boldsymbol{\delta}_1\right](f^\dagger_{\mathrm{B}\mathbf{k}_1\alpha}f^\dagger_{\mathrm{A}\mathbf{k}_2\gamma}f_{\mathrm{A}\mathbf{k}_3\delta}f_{\mathrm{B}\mathbf{k}_4\beta} + f^\dagger_{\mathrm{A}\mathbf{k}_1\alpha}f^\dagger_{\mathrm{B}\mathbf{k}_2\gamma}f_{\mathrm{B}\mathbf{k}_3\delta}f_{\mathrm{A}\mathbf{k}_4\beta})\Big), \quad (36a)$$

$$P^y = \frac{2\sqrt{3}ieat^3}{U^3}\sum_{\{\mathbf{k}\}}{}' \delta_{\alpha\beta\gamma\delta}\Big(2\sin[-\mathbf{k}_1\cdot\boldsymbol{\delta}_2 + \mathbf{k}_2\cdot\boldsymbol{\delta}_3 - \mathbf{k}_3\cdot\boldsymbol{\delta}_3 + \mathbf{k}_4\cdot\boldsymbol{\delta}_2]\left(f^\dagger_{\mathrm{A}\mathbf{k}_1\alpha}f^\dagger_{\mathrm{B}\mathbf{k}_2\gamma}f_{\mathrm{B}\mathbf{k}_3\delta}f_{\mathrm{A}\mathbf{k}_4\beta} + f^\dagger_{\mathrm{B}\mathbf{k}_1\alpha}f^\dagger_{\mathrm{A}\mathbf{k}_2\gamma}f_{\mathrm{A}\mathbf{k}_3\delta}f_{\mathrm{B}\mathbf{k}_4\beta}\right) +$$
$$\sin[\mathbf{k}_1\cdot\boldsymbol{\delta}_3 + \mathbf{k}_2\cdot\boldsymbol{\delta}_1 - \mathbf{k}_3\cdot\boldsymbol{\delta}_1 - \mathbf{k}_4\cdot\boldsymbol{\delta}_3]\left(f^\dagger_{\mathrm{B}\mathbf{k}_1\alpha}f^\dagger_{\mathrm{B}\mathbf{k}_2\gamma}f_{\mathrm{B}\mathbf{k}_3\delta}f_{\mathrm{B}\mathbf{k}_4\beta} + f^\dagger_{\mathrm{A}\mathbf{k}_1\alpha}f^\dagger_{\mathrm{A}\mathbf{k}_2\gamma}f_{\mathrm{A}\mathbf{k}_3\delta}f_{\mathrm{A}\mathbf{k}_4\beta}\right) -$$
$$\sin[\mathbf{k}_1\cdot\boldsymbol{\delta}_1 + \mathbf{k}_2\cdot\boldsymbol{\delta}_2 - \mathbf{k}_3\cdot\boldsymbol{\delta}_2 - \mathbf{k}_4\cdot\boldsymbol{\delta}_1]\left(f^\dagger_{\mathrm{B}\mathbf{k}_1\alpha}f^\dagger_{\mathrm{A}\mathbf{k}_2\gamma}f_{\mathrm{A}\mathbf{k}_3\delta}f_{\mathrm{B}\mathbf{k}_4\beta} + f^\dagger_{\mathrm{A}\mathbf{k}_1\alpha}f^\dagger_{\mathrm{B}\mathbf{k}_2\gamma}f_{\mathrm{B}\mathbf{k}_3\delta}f_{\mathrm{A}\mathbf{k}_4\beta}\right)\Big). \quad (36b)$$

[1] S. Banerjee, U. Kumar, and S.-Z. Lin, Phys. Rev. B **105**, L180414 (2022).
[2] J.-Y. P. Delannoy, M. J. P. Gingras, P. C. W. Holdsworth, and A.-M. S. Tremblay, Phys. Rev. B **72**, 115114 (2005).
[3] T. Cookmeyer, J. Motruk, and J. E. Moore, Phys. Rev. Lett. **127**, 087201 (2021).
[4] O. I. Motrunich, Phys. Rev. B **73**, 155115 (2006).
[5] B.-B. Chen, Z. Chen, S.-S. Gong, D. N. Sheng, W. Li, and A. Weichselbaum, Phys. Rev. B **106**, 094420 (2022).
[6] W. X. Gang, *Quantum field theory of many-body systems* (Oxford University Press, Oxford, 2007).
[7] F. Oliviero, J. A. Sobral, E. C. Andrade, and R. G. Pereira, SciPost Phys. **13**, 050 (2022).
[8] E. H. Lieb, Phys. Rev. Lett. **73**, 2158 (1994).
[9] T. Fukui, Y. Hatsugai, and H. Suzuki, J. Phys. Soc. Japan **74**, 1674 (2005).
[10] L. N. Bulaevskii, C. D. Batista, M. V. Mostovoy, and D. I. Khomskii, Phys. Rev. B **78**, 024402 (2008).